Fluorescent bio/chemosensors based on silole and tetraphenylethene luminogens with aggregation-induced emission feature

Ming Wang,[a] Guanxin Zhang,[a] Deqing Zhang,*[a] Daoben Zhu*[a] and Ben Zhong Tang*[b]

Received 19th October 2009, Accepted 19th November 2009
First published as an Advance Article on the web 21st January 2010
DOI: 10.1039/b921610c

New fluorescent sensors have been developed, utilizing the aggregation-induced emission (AIE) attribute of silole and tetraphenylethene luminogens. In this feature article, we briefly summarize recent progress in the development of AIE-based bio/chemosensors for assays of nuclease and AChE activities, screening of inhibitors, and detection of various analytes including charged biopolymers, ionic species, volatile and explosive organic compounds.

1. Introduction

It is well known that light emissions of many organic and polymeric fluorophores are quenched when their solution concentrations are increased and when they are aggregated in the solid state (aggregation-caused quenching or ACQ), due to the formation of such detrimental species as excimers and exciplexes.[1] The notorious ACQ effect has greatly limited the scope of the applications of the fluorophores as sensory materials, especially in the area of biomolecule assays in the aqueous media because 1) the fluorophores aggregate in the polar media, which weakens their light emissions and 2) the fluorophores tend to aggregate in the hydrophobic pockets of the folding structures of biopolymers, leading to fluorescence quenching. The fluorescence resonance energy transfer (FRET) mechanism has been widely used to avoid the ACQ effect in the design of new fluorescent biosensors.[2] In this approach, however, fluorophore-labeled biomolecules need to be prepared, which often require nontrivial synthetic efforts and involve painstaking isolation and purification procedures.[3]

It is interesting to note that some organic molecules behave "abnormally": they are practically non-luminescent in the solution state but become strongly emissive when aggregated. This unusual fluorescence phenomenon was referred as to "aggregation-induced emission" (AIE). In 2001, we observed such AIE effect in 1-methyl-1,2,3,4,5-pentaphenylsilole (**1**; Scheme 1).[4] We later found that tetraphenylethene (TPE; **2**) and its derivatives also showed AIE behavior.[5]

Experimental and theoretical investigations indicated that the intramolecular rotations in the AIE molecules would deactivate

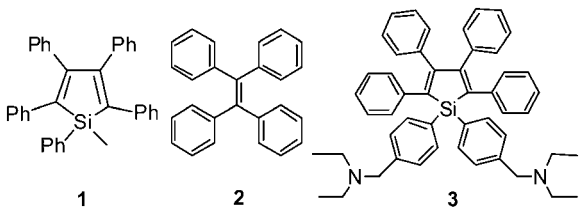

Scheme 1 Chemical structures of representative examples of silole and TPE luminogens showing the aggregation-induced emission (AIE) phenomenon.

[a]*Organic Solids Laboratory, Institute of Chemistry, Chinese Academy of Sciences, Beijing, 100190, China. E-mail: dqzhang@iccas.ac.cn*
[b]*Department of Chemistry, The Hong Kong University of Science & Technology (HKUST), Clear Water Bay, Kowloon, Hong Kong, China. E-mail: tangbenz@ust.hk*

Ming Wang

Ming Wang was born in 1982 and received his B.S. in chemistry from Anqing Normal College in Anhui Province in 2002 and Ph.D. degree in organic chemistry from Institute of Chemistry, Chinese Academy of Sciences (ICCAS) in 2009. His research interests include the design and synthesis of organic functional molecules and optical chemo/biosensors.

Guanxin Zhang

Guanxin Zhang was born in 1976 and received his masters degree in chemistry from Beijing Normal University in 2002 and Ph.D. degree in organic chemistry from ICCAS in 2005. His research interests include the design, synthesis and self-assembly of organic functional molecules, optical chemol biosensors and nanomaterials.

the corresponding excited states, thus making them non-emissive in the respective solutions.[6] The intramolecular rotations are restricted in the aggregate states and as a result their emissions are enhanced.[6] In silole **1** and its analogues, excimers are unlikely to form due to their propeller-like molecular conformations and their emissions are thus not quenched in the aggregate state. Taking advantage of the unusual fluorescence effect, highly efficient organic light-emitting diodes (OLEDs) using AIE molecules as emitters have been fabricated.[7]

The AIE luminogens have also been utilized for the design and preparation of sensitive and selective bio/chemosensors. By proper structural modifications to the AIE molecules, their aggregation states can be influenced by the analytes through electrostatic attraction, coordination binding, *etc.* In this way, new fluorescence analysis methods can be established for the detection of biomacromolecules (*e.g.*, protein, heparin and DNA),[8,9] assays of nuclease and acetylcholinesterase (AChE) activities and screening of inhibitors[10–12] as well as probing of ionic species.[13–15] In this feature article, we give an account of the recent advances in the constructions of silole- and TPE-based bio/chemosensors. We demonstrate that AIE offers a new platform for the development of new sensing systems.

2. Detection of charged biomolecules

Silole derivative **3** (Scheme 1) was prepared by attaching two amino groups to the *para*-positions of the 1,1-diphenyl rings of hexaphenylsilole. The possibilities of using **3** as chemo- and biosensors for monitoring pH changes and detecting biological macromolecules were explored. Silole **3** is AIE active and shows strong emission when its nanoaggregates are suspended in a THF and water mixture. When acid is added to the mixture, the suspension becomes non-fluorescent again, for the amino groups in **3** are transformed to ammonium salts in the presence of acid. We further examined the application of **3** as a biosensor in the acidic mixture. Silole **3** contains positively charged ammonium groups and may bind to negatively charged biomolecules *via* electrostatic interaction. Whereas the buffer solution (pH = 2.0) of **3** emits weakly, addition of bovine serum albumin (BSA) or herring sperm (hs) DNA to the solution causes **3** to resume its emission, whose intensity is increased with increasing the concentration of BSA or (hs)DNA.[8] Evidently, **3** can be utilized as a fluorescence "turn-on " biosensor for protein and DNA.

Silole **4** (Scheme 2) possesses an ammonium group and is positively charged independent of the pH value of the solution. It is expected that co-aggregation of silole **4** with negatively-charged biomolecules through electrostatic interactions will occur and as a result the fluorescence of silole **4** will be enhanced in the presence of these biomolecules.

Accordingly, **4** can be utilized for detection of negatively charged biomolecules. Heparin is a highly sulfated linear glycoaminoglycan (GAG; Scheme 2). It is crucial to monitor and control the level and activity of heparin during and after surgery and to manipulate the amount of heparin for anti-coagulant therapy in order to avoid the complications such as hemorrhage

Deqing Zhang

Deqing Zhang obtained his masters degree in organic chemistry from Institute of Chemistry, ICCAS in 1990. He received his Ph.D. degree from Ruprecht-Karls University Heidelberg in 1996 under the supervision of Prof. Dr H. A. Staab. Now he is a research Professor in ICCAS. His research interests include the development of external stimuli-responsive molecular systems for molecular switches, logic gates and chemo/biosensors. He also shows interest in design and synthesis of organic functional materials and organic nanoassemblies. He serves as editorial advisory board member of a few scientific journals including Langmuir and Dyes and Pigments.

Daoben Zhu

Daoben Zhu finished his graduate courses at the East China University of Science and Technology in 1968. Currently, he is a research professor and director of the Organic Solids Laboratory in ICCAS. He was elected as an academician of CAS in 1997. His research mainly focuses on molecular materials and devices. He is vice-president of Chinese Chemical Society and vice-president of Chinese Materials Society. He serves as editorial board and international advisory board member of several journals including Applied Physics A, Chemistry-An Asian Journal, Macromolecular Rapid Communications, Polymer Reviews and Molecular Physics Reports.

Ben Zhong Tang

Ben Zhong Tang received his Ph.D. from Kyoto University and conducted postdoctoral work at University of Toronto. He joined HKUST in 1994 and was promoted to Chair Professor in 2008. He is interested in creating new molecules with novel structures and unique properties. He received a Natural Science Award from Chinese Government and a Senior Research Fellowship from Croucher Foundation in 2007. He is a science news contributor to Noteworthy Chemistry (ACS) and is a member of the editorial boards of several scientific journals, including Progress in Polymer Science (Elsevier), Polymer Chemistry (RSC), and Macromolecules (ACS). He was elected to the Chinese Academy of Sciences in 2009.

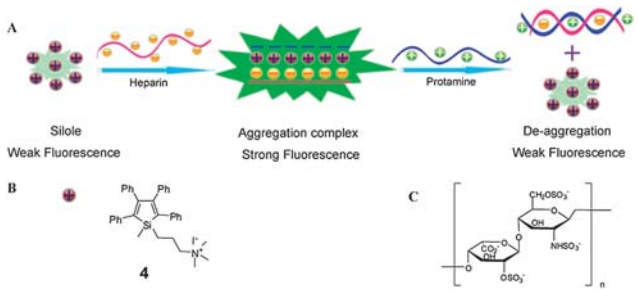

Scheme 2 Chemical structures of silole **4** and heparin and illustration of the working principle for the detection of heparin with silole **4**.

or thrombocytopenia induced by overdose of heparin.[16] As anticipated, **4** is weakly emissive in the buffer solution, but its fluorescence intensity is increased gradually upon addition of heparin as shown in Fig. 1. The fluorescence enhancement of **4** upon mixing with heparin can be easily distinguished with the naked eye under UV illumination as shown in the inset of Fig. 1. Moreover, it is possible to analyze heparin in the serum with **4** as its emission intensity increases linearly with the concentration of heparin present in the serum and the interference of other biomolecules in the serum can be neglected by lowering the pH value. Therefore, a convenient fluorescence "turn-on" detection of heparin can be established with silole **4**.

Additionally, silole **4** can be a potentially useful fluorescent probe for investigating the interactions of heparin with specific proteins.[17] Fig. 2 shows the fluorescence change of **4** in the presence of heparin and protamine. The fluorescence intensity of **4** is increased when heparin is added. However, when protamine is added into the mixture, the fluorescence intensity starts to decrease, eventually reaching the intensity of the solution of **4** in the absence of heparin and protamine. The fluorescence decrease indicates that the interaction between heparin and protamine has induced the ensemble of **4** and heparin to deaggregate (Scheme 2).

Charged TPE derivatives (Scheme 3) are also investigated for the detection of biomolecules. The luminogen containing two ammonium groups (**5**) emits weakly, but its fluorescence is

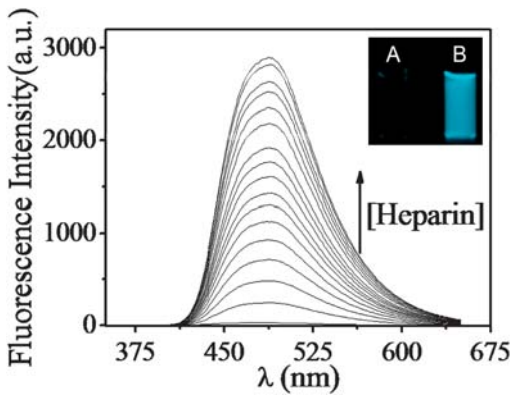

Fig. 1 Fluorescence spectra of compound **4** (5.0×10^{-5} M in HEPES buffer solution, pH = 7.4) in the presence of different amounts of heparin (from 0 to 13 μM); inset shows photographs of the solution of **4** in the absence (A) and presence (B) of heparin (7 μM) under UV (365 nm) illumination.

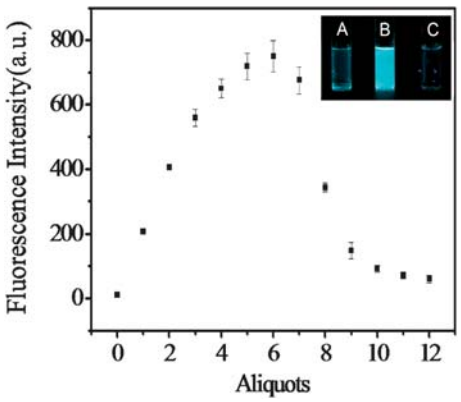

Fig. 2 Variation of the fluorescence intensity of **4** (1.25×10^{-5} M in HEPES buffer solution, pH = 7.4) after addition of heparin (0–3.0 μM), followed by addition of protamine ($0–5.2 \times 10^{-3}$ mg mL^{-1}); inset shows photographs of the solution of **4** (1.25×10^{-5} M) under UV (365 nm) illumination: (A) in the absence of heparin and protamine; (B) in the presence of heparin (4.0 μM); (C) in the presence of heparin (4.0 μM) and protamine (2.8×10^{-2} mg mL^{-1}).

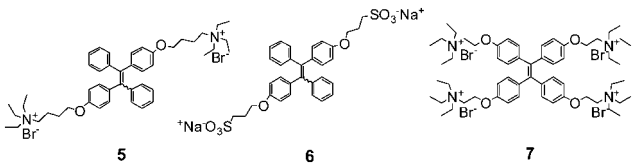

Scheme 3 The chemical structures of TPE compounds **5**, **6** and **7**.

turned on after addition of negatively charged biomolecules such as calf thymus (ct) DNA and BSA.[5] It is believed that the electrostatic and hydrophobic interactions between **5** and the biomolecules induce the formation of aggregation complexes and consequently the fluorescence enhancement.

The negatively charged TPE derivative **6** (Scheme 3) can be utilized to study the unfolding process of BSA in the presence of surfactants [*e.g.* sodium dodecyl sulfate (SDS)]. It is found that addition of BSA to the solution of **6** leads to fluorescence increase. This is likely due to the entrance of the molecules of **6** into the hydrophobic pockets of the native folding structure of BSA. The rotation of the σ-bands within the TPE unit is frozen, resulting in the emission enhancement.[18] The solution of **6** and BSA became almost non-fluorescent again after addition of SDS. SDS induces unfolding of BSA chains and accordingly the hydrophobic pockets within the folding structure of BSA are not available for interaction with molecules of **6**.

We have recently showed that TPE derivative **7** (Scheme 3) with four positive charges can be used as a fluorescence label-free DNA conformation sensor.[19] It is known that DNA with a guanine-rich sequence changes its conformation from random-coil to G-quadruplex structure in the presence of a stabilizer. The research on G-quadruplex has received great attention since it is relevant to the elongation of telomeres in immortalized and most tumor cells.[20] Inhibition of telomerase activity through stabilization of the G-quadruplex structure is thus considered to have potential application in drug design.[21] As anticipated, the fluorescence of **7** is turned on when mixed with either random-coil or

G-quadruplex DNA. Interestingly, a red shift in the fluorescence spectrum of **7** is observed when the DNA conformation is transformed from random-coil to G-quadruplex. This spectral feature enables **7** to be used to monitor the folding process of guanine-rich DNA strands and to screen G-quadruplex stabilizers.

3. Nuclease activity assay and inhibitor screening

Nucleases that can catalyze the hydrolysis of DNA into mono- or oligonucleotide fragments play important roles in biological processes and show wide applications in biotechnology; thus, development of simple and convenient fluorescent sensors for DNA detection and nuclease assay will be of great importance in diagnosing genetic diseases and monitoring biological processes in the cell. Various fluorescent probes for DNA detection and nuclease activity assay have been reported.[22,23] Taking advantage of the AIE feature of silole compounds, a label-free fluorescence nuclease assay can be constructed with silole **4** (Scheme 2).[10]

Fig. 3 shows the fluorescence enhancement of silole **4** after the addition of 15-mer single-strand DNA (ssDNA). For instance, the fluorescence intensity of the buffer solution of silole **4** was enhanced by 27 times in the presence of 0.3 μM of ssDNA (15-mer). It is interesting to note that the fluorescence intensity of silole **4** increases almost linearly with the concentration of ssDNA. Thus, a fluorescence turn-on detection of ssDNA can be achieved with silole **4**.[10] However, such fluorescence enhancement observed for silole **4** was found to be dependent on the length of ssDNA; the longer the ssDNA strand, the more significantly increases the fluorescence of silole **4**. These results are understandable by considering the fact that the longer DNA strand provides more negative charge sites to interact with the ammonium group in silole **4**, thus leading to strong aggregation of the molecules of silole **4**, while the short DNA can only offer limited negative sites for interactions with silole **4** and as a result stable aggregation complex can not be formed. This offers an attractive possibility to employ **4** to follow the DNA cleavage process. Indeed, the fluorescence of the ensemble of silole **4** and ssDNA was rather strong; however, if ssDNA was pre-treated with Fenton's reagent that generates HO$^{\bullet}$ to cleave DNA into fragments, the fluorescence of ensemble became very weak.

Silole **4** can be employed to study the DNA cleavage catalyzed by nucleases.[10] The ensemble of silole **4** and ssDNA exhibits rather strong fluorescence before the reaction of DNA with nuclease. However, as can be seen from Fig. 4 the fluorescence of the ensemble is reduced after DNA cleavage by nuclease, and the fluorescence intensity of the ensemble decreases gradually by prolonging the reaction time. The cleavage reaction was carried out at different concentrations of the nuclease and ssDNA in the presence of silole **4**. The results show that the fluorescence intensity of silole **4** decreases rapidly for the cleavage reaction with high concentration of nuclease. This is indeed in agreement with the fact that the ssDNA cleavage reaction becomes fast by increasing the concentration of nuclease. By varying the DNA concentration in the reaction mixture, the kinetic parameters, Michaelis constant (K_m) and maximum of initial reaction rate (V_{max}) for the nuclease-catalyzed hydrolysis reaction can be determined by fitting the corresponding fluorescence spectral data with the Michalis–Menten equation. The values of K_m and V_{max} obtained by using silole **4** as a fluorescent probe are comparable to those obtained with other methods. These results clearly manifest that a label-free fluorescence nuclease activity assay can be established with silole **4** and its analogues.

This new fluorescence label-free nuclease assay method can also be employed for screening the inhibitors.[10] Pyrophosphate, a typical nuclease S1 inhibitor,[23] was used as an example to demonstrate the usefulness of silole **4** for screening inhibitors of nucleases. Fig. 5 shows the variation of the fluorescence intensity of the ensemble of silole **4**, ssDNA and nuclease in the absence and presence of pyrophosphate *vs.* the reaction time. Obviously, the decrease in the fluorescence intensity of the ensemble is much slower in the presence of pyrophosphate, compared to that in the absence of pyrophosphate. This result implies that pyrophosphate can prohibit the hydrolysis reaction catalyzed by nuclease S1, and this is fully in accordance with the fact that pyrophosphate is known as a nuclease S1 inhibitor. It may be concluded that this method can be extended to other nuclease assays and

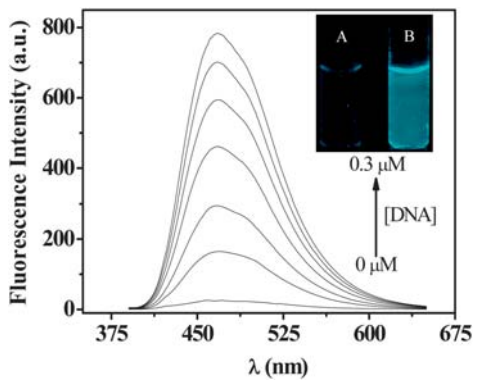

Fig. 3 The fluorescence spectra of **4** (2.0×10^{-5} M in 20 mM tris buffer solution, pH = 7.3) in the presence of different amounts of 15-mer ssDNA (from 0 to 0.3 μM); inset shows the photographs of the solution of **4** in the absence (A) and presence (B) of ssDNA (0.3 μM) under UV light (365 nm) illumination.

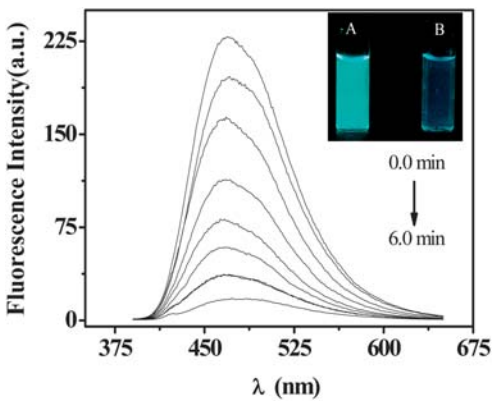

Fig. 4 Fluorescence spectrum of **4** (2×10^{-5} M in 20 mM tris buffer solution, pH = 7.3) containing 15-mer ssDNA (5.0 μM) and those after cleavage by nuclease S1 for different periods; inset shows the photographs of the solution of **4** (2×10^{-5} M) in the presence of ssDNA (5 μM) (A) and cleaved ssDNA by nuclease S1 (50 U/mL) for 10 min (B) under UV light (365 nm) illumination.

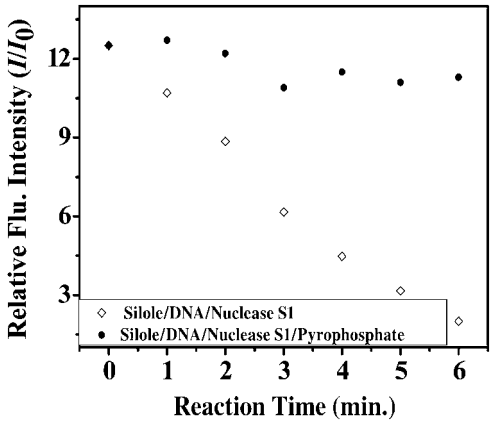

Fig. 5 Inhibition effect of pyrophosphate on 15-mer ssDNA cleavage by nuclease S1 monitored by fluorescence variation of silole **4**.

high-throughput screening of nuclease inhibitors, given its simplicity, easy-operation, sensitivity and cost-effectiveness.

4. Selective ATP detection and relevant phosphatase assay

Adenosine 5′-triphosphate (ATP),[24] one of the most important molecules involved in many biological processes, shows close relations to many diseases such as ischemia, Parkinson's disease and hypoglycemia.[25] The development of a selective detection method for ATP is thus of obvious importance. We have found that the fluorescence of **4** increases after addition of ATP. Of particular interest is that almost no fluorescence enhancements are observed for adenosine 5′-diphosphate (ADP), adenosine 5′-monophosphate (AMP), and inorganic pyrophosphate (PPi), as shown in Fig. 6. Accordingly, silole **4** can be employed to selectively detect ATP. Such a fluorescence increase observed for silole **4** can be understood as follows: 1) ATP possesses more negative charges compared to ADP and AMP, and less charged ADP and AMP may not be able to form stable aggregation complexes with silole **4**; 2) although ATP and PPi have the same

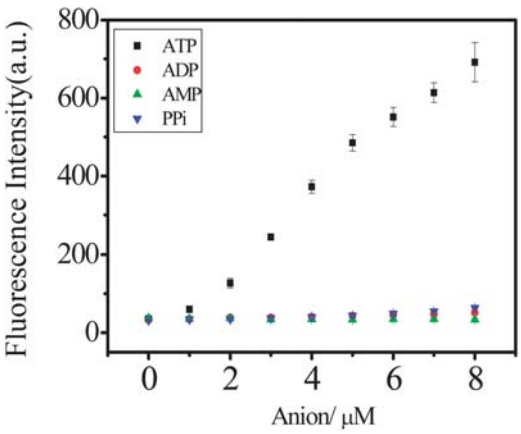

Fig. 6 Variation of the relative fluorescence intensity of silole **4** (8×10^{-5} M in 10 mM, pH = 9.0 tris buffer solution) *vs.* the respective concentrations of ATP, ADP, AMP and pyrophosphate; the fluorescence was monitored at 470 nm by excitation at 370 nm.

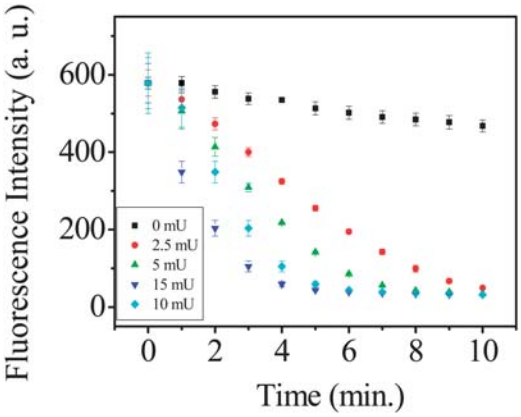

Fig. 7 The plot of the fluorescence intensity at 470 nm of silole **4** [8×10^{-5} M in tris buffer solution (10 mM, pH = 9.0)] containing ATP (5.0 μM) *vs.* the hydrolysis reaction time for selected concentrations of CIAP.

negative charges, the hydrophobic interaction between the adenosine group in ATP and the tetraphenylsilole group in **4** may also contribute to the formation of an aggregation complex.

The enzyme-catalyzed ATP hydrolysis into ADP/AMP is one of the most important biological reactions. By making use of the ability of silole **4** to discriminate ATP, ADP and AMP, silole **4** was utilized as a fluorescence probe for *in situ* and continuous monitoring of the ATP hydrolysis.[26] As displayed in Fig. 7, the fluorescence intensity of the ensemble of silole **4** and ATP decreased gradually after addition of calf intestinal alkaline phosphatase (CIAP), which can catalyze the ATP hydrolysis; high concentration of CIAP in the ensemble led to a rapid fluorescence reduction. As for the DNA nucleases silole **4** can also be utilized for screening the CIAP inhibitors.

5. Acetylcholinesterase activity assay and inhibitor screening

Acetylcholine is a central neurotransmitter, whose hydrolysis catalyzed by AChE is a key process for the regulation of the neuro-response system. It is accepted that Alzheimer's disease (AD) is related to a low level of acetylcholine in the brain.[27] Accordingly, current rational pharmacological strategies for AD are mostly based on cholinergic hypothesis. In addition, nerve gases and some pesticides[28,29] are inhibitors of AChE. An efficient assay method for AChE activity will thus be useful for detecting these nerve gases and pesticides.

A number of methods have been described for AChE activity assay. These include a colorimetric method based on Ellman's reagent, fluorescence approaches and chemiluminescent probes.[30] Colorimetric gold nanoparticles[31] and fluorometric CdS quantum dots[32] are also successfully employed for inhibition studies of AChE. However, drawbacks are found for these assay methods. Therefore, it is still highly desirable to develop convenient, fast, and continuous analytical methods for AChE activity assay and inhibitor screening.

We have recently reported a new, convenient, continuous fluorometric assay method for AChE based on an AIE dye.[11] TPE luminogen **6** (Scheme 3) is a sodium salt carrying two sulfonate ($-SO_3^-$) units, and it is expected that it emits weakly in

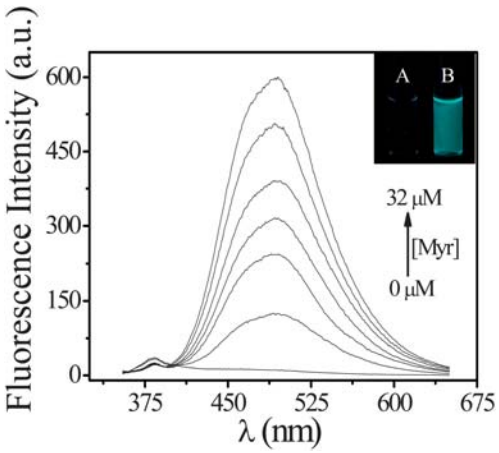

Fig. 8 Fluorescence spectra of **6** [20 μM in PBS (10 mM) buffer solution, pH = 8.0] in the presence of different amounts of myristoylcholine (from 0 to 32 μM); inset shows the photographs of the corresponding buffer solutions of **6** (20 μM) in the absence (A) and presence (B) of myristoylcholine (32 μM) under UV light (365 nm) illumination.

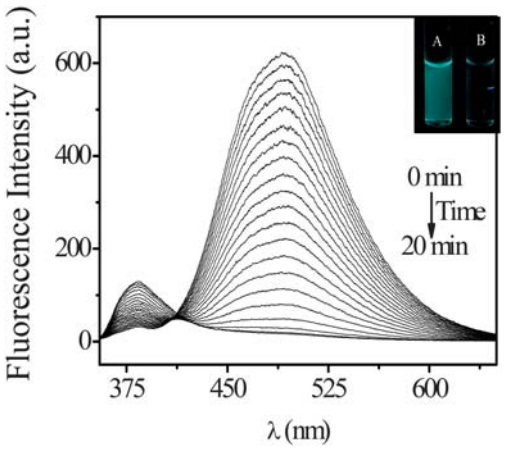

Fig. 9 Fluorescence spectra of the ensemble of **6** (20 μM in PBS buffer solution, pH = 8.0) and myristoylcholine (25 μM) in the presence of AChE (0.5 U mL^{-1}) incubated for different periods; inset shows the photographs of the corresponding solutions of **6** and myristoylcholine without (A) and with (B) AChE (0.5 U mL^{-1}) after 15 min incubation under UV light (365 nm) illumination.

aqueous solution. Addition of myristoylcholine, an amphiphilic compound, to the solution of **6** induces emission enhancement as shown in Fig. 8. Fluorescence confocal microscopic and dynamic light scattering (DLS) studies reveal the formation of fluorescent aggregates which are assumed to be supramolecular hetero-aggregation complexes formed between **6** and myristoylcholine *via* electrostatic interactions as illustrated in Scheme 4.

It is known that myristoylcholine can easily be hydrolyzed into myristic acid and choline in the presence of AChE.[33] Addition of AChE to the ensemble of **6** and myristoylcholine led to fluorescence reduction as shown in Fig. 9. This is probably due to the disassembly of the aggregative complexes of compound **6** and myristoylcholine formed because of the coulombic repulsive interaction between **6** and the hydrolysis product of myristoylcholine as schematically shown in Scheme 4. The fluorescence variation of the ensemble of **6**, myristoylcholine and AChE is found to be dependent on the concentrations of myristoylcholine and AChE. Based on these fluorescent spectral data the kinetic parameters, Michaelis constant (K_m) and maximum of initial reaction rate (V_{max}) for AChE-catalyzed hydrolysis of myristoylcholine, were determined to be 24.4 μM and 7.66 μM min^{-1}, respectively. It should be noted that the K_m value determined herein using the AIE-based assay method and myristoylcholine as substrate is close to those reported earlier by using a microfluidic assay method and Ellman assay in which acetylthiocholine was chosen as AChE substrate.[34]

In addition, this AIE-based AChE assay method can also be utilized for AChE inhibitor screening.[11] 9-Amino-1,2,3,4-tetrahydroacridine (tacrine), a typical inhibitor for AChE,[35] is selected as an example to demonstrate the usefulness of **6** for AChE inhibitor screening. As expected, the fluorescence reduction for the ensemble of **6** and myristoylcholine after addition of AChE becomes small in the presence of tacrine, since tacrine can inhibit the AChE activity. Using this AIE assay method, the IC_{50} of tarcine toward AChE is estimated to be 159 nM, being close to that obtained with commonly used Ellman's reagent (IC_{50} = 108 nM).[34]

An alternative fluorescence turn-on assay method for AChE activity and the inhibitor screening is based on the ensemble of **6** and **8** (Scheme 5).[12] This assay is designed on the basis of the

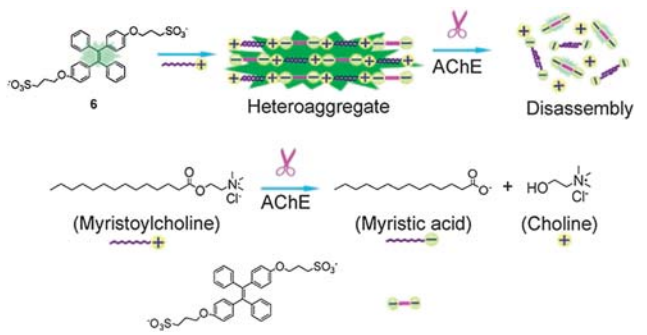

Scheme 4 Illustration of a new fluorometric AChE assay method based on the AIE feature of TPE luminogen **6**.

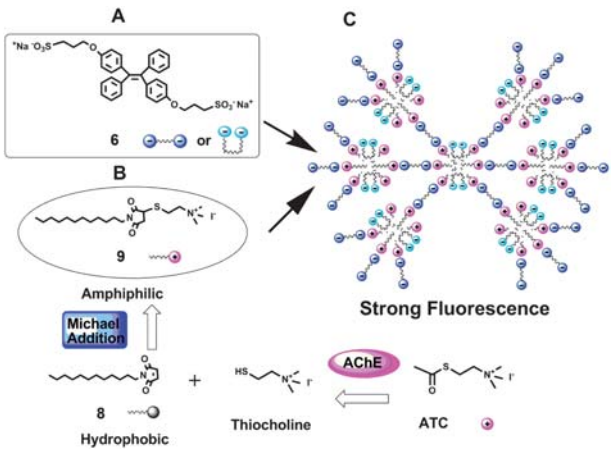

Scheme 5 Illustration of fluorescence turn-on assay method for acetylcholinesterase activity using TPE luminogen **6**.

following considerations. 1) Acetylthiocholine iodide (ATC) is a good substrate of AChE. In other words, ATC can be hydrolyzed into thiocholine in the presence of AChE. Michael reaction of thiocholine with the maleimide group in **8** would lead to the formation of an amphiphilic compound **9**. 2) Such an amphiphilic compound would induce the molecules of **6** to aggregate and accordingly the fluorescence of the ensemble would increase significantly.

The fluorescence of the ensemble of molecules of **6**, **8** and ATC increases gradually after introducing AChE, as shown in Fig. 10. Moreover, the fluorescence of the ensemble increases more significantly when the concentration of AChE is high in the ensemble. Similarly, the ensemble of **6**, **8** and ATC can be utilized for screening the inhibitors of AChE. Addition of neostigmine/tacrine/donepezil, which are inhibitors of AChE, to the ensemble of **6**, **8** and ATC induces a small fluorescence enhancement after introducing AChE to the ensemble. Their IC_{50} values are estimated with this fluorescence turn-on method, which are similar to those obtained with other assay methods. Therefore, by making use of the AIE feature of **6** and the cascade reactions among acetylthiocholine, AChE and **8**, another new fluorescence "turn-on" method is developed for AChE assay and inhibitor screening.

6. Selective detection of specific anions and metal cations

Cyanide is one of the most toxic anions and harmful to human health and the environment.[36] By making use of the coordination ability and nucleophilic reactivity of cyanide, a number of chemical sensors for cyanide have been developed.[37] For instance, Sessler *et al.* have recently described a selective cyanide indicator based on the benzyl-cyanide reaction.[37a] However, drawbacks exist for these cyanide sensors. These include poor selectivity, and the fact that the detection of cyanide cannot be performed in aqueous solution in some cases. Fluorescent probes for cyanide are reported,[37b,7c] but fluorescence turn-on detection still remains rare.

We have recently developed a fluorescence turn-on sensing ensemble for cyanide in aqueous solution by making use of the AIE feature of silole luminogens. The working mechanism for this cyanide sensor is illustrated in Scheme 6. Briefly, the nucleophilic addition of cyanide to the trifluoroacetylamino group in **10** yields an amphiphilic species[37] that would induce the aggregation of silole **4**, and as a result the fluorescence of the ensemble increases greatly. As anticipated, the ensemble of **4** and **10** displayed rather weak fluorescence, which is increased gradually after addition of cyanide, as shown in Fig. 11. The detection limit of cyanide using with this ensemble was estimated to be 7.74 μM, which is lower than the concentration of cyanide in the blood of fire victims. Interference experiments with other anions including AcO^-, Br^-, Cl^-, F^-, $H_2PO_4^-$, HSO_4^-, N_3^- and NO_3^- reveal that the ensemble of **4** and **10** is selective toward cyanide anions over other common inorganic anions.

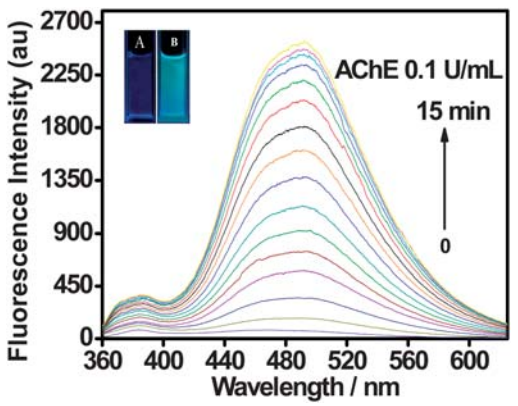

Fig. 10 Fluorescence spectra of the ensemble of **6** [20 μM in HEPES (10 mM) buffer solution, pH = 7.35], compound **8** (30 μM) and ATC (30 μM) in the presence of AChE (0.1 U mL^{-1}) incubated at room temperature for different periods; inset shows the photographs of the corresponding mixed buffer solution in the absence (A) and presence (B) of AChE (0.1 U mL^{-1}) after incubation for 15.0 min under UV light (365 nm) illumination.

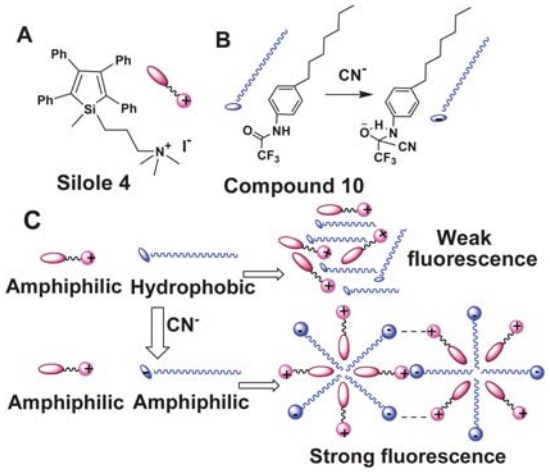

Scheme 6 Illustration of the design rationale for the fluorescent cyanide sensor based on the AIE feature of silole **4**.

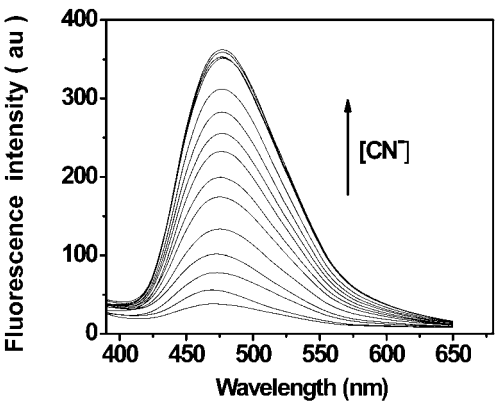

Fig. 11 Fluorescence spectra of the ensemble of silole **4** (7.5×10^{-5} M) and compound **10** (4.0×10^{-4} M) in DMSO/H_2O (1/75, v/v) in the presence of different concentrations of sodium cyanide (from 0 to 14×10^{-5} M).

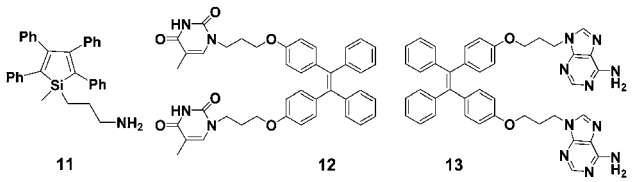

Scheme 7 Silole and tetraphenylethylene compounds **11**, **12** and **13** for the detection of CrO_4^{2-}, AsO_4^{3-}, Hg^{2+} and Ag^+.

CrO_4^{2-} and AsO_4^{3-} anions are also harmful to environment and human health. Trogler *et al.*[14] utilized nanoparticles of **11** (Scheme 7) for sensing CrO_4^{2-}/AsO_4^{3-}. The nanoparticles are formed by injection of water into the THF solution of **11**. The nanoparticles show strong fluorescence due to the AIE feature of **11**. The fluorescence of the nanoparticles is gradually quenched by addition of CrO_4^{2-}/AsO_4^{3-}. Such quenching is ascribed to the electron transfer from the excited state of **11** to CrO_4^{2-}/AsO_4^{3-}. As low as 0.1 ppm of CrO_4^{2-} can be detected with the nanoparticles of **11**. Common anions such as NO_3^-, NO_2^-, SO_4^{2-} and ClO_4^- do not interfere with the detection.

Hg^{2+} and its compounds are severe environmental pollutants and several diseases are known to be associated with mercury contamination. Ag^+ and its compounds also have adverse biological effects and there are many reports on silver bioaccumulation and toxicity. Thus, the development of sensitive and selective chemosensors for Hg^{2+} and Ag^+ in various media is of considerable importance for environment protection and human health. Traditional quantitative approaches to Hg^{2+} and Ag^+ detection are expensive and time-consuming in practice.[38] In comparison, sensitive and selective optical sensors for Hg^{2+} and Ag^+ with simple instrumental implementation and easy operation have received a lot of attention. Up to now, only a few fluorescence "turn on" chemosensors for Hg^{2+} and Ag^+ have been described[39] as both Hg^{2+} and Ag^+ as heavy transition metal (HTM) ions are known as fluorescence quenchers.

We have developed fluorescence "turn on" chemosensors for Ag^+ and Hg^{2+} by making use of the unique AIE feature of the TPE motif and the selective binding abilities of thymine (with Hg^{2+}) and adenine (with Ag^+).[15] The design rationale is illustrated in Scheme 8. In brief, **12** and **13** contain two thymine and adenine units, respectively. The coordination of thymine and adenine with Hg^{2+} and Ag^+, respectively, would induce the formation of extended coordination complexes and as a result, the aggregation of TPE units in **12** and **13** would occur. As shown

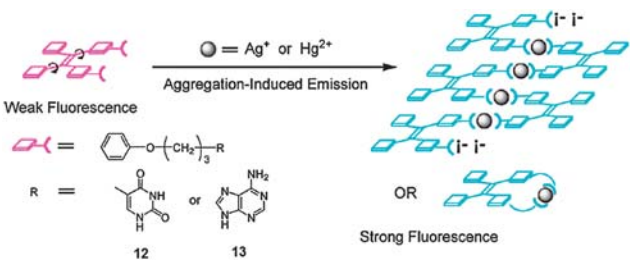

Scheme 8 Illustration of the design rationale for the Ag^+ and Hg^{2+} fluorescence turn-on chemosensors based on TPE luminogens containing thymine (**12**) and adenine (**13**) units.

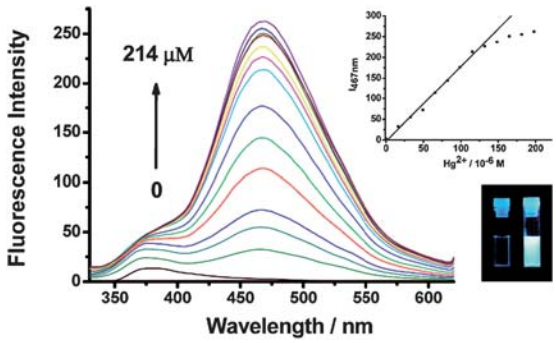

Fig. 12 Fluorescence spectra of compound **12** (1.34×10^{-4} M in H_2O–CH_3CN (2 : 1, v/v) in the presence of increasing amounts of $Hg(ClO_4)_2$ (from 0 to 214 μM); inset shows (1) the plot of the fluorescence intensity (I_{467nm}) *vs.* the concentration of $Hg(ClO_4)_2$; (2) the photographs of the solution of **12** before and after addition of 1.0 equiv of $Hg(ClO_4)_2$ under UV light illumination (365 nm).

in Fig. 12, addition of $Hg(ClO_4)_2$ to the solution of **12** leads to the emergence of the emission around 467 nm and its intensity is increased linearly with the concentration of Hg^{2+} in the range of 0–125 μM. Hg^{2+} with concentration as low as 0.37 μM can be detected with **12**. Other metal ions including Ba^{2+}, Ca^{2+}, Cd^{2+}, Co^{2+}, Cu^{2+}, Fe^{3+}, Fe^{2+}, Mg^{2+}, Mn^{2+}, Ni^{2+}, Pb^{2+}, Zn^{2+}, Ag^+, Cs^+ and K^+ exert no interference with the detection of Hg^{2+} with **12**. Similar results are obtained when **13** is used to detect Ag^+. In this case, however, Hg^{2+} interferes slightly with the detection of Ag^+ by **13**.

Detection of volatile and explosive organic compounds

There are several reports about the application of AIE-active silole and TPE luminogens in the detection of volatile organic compounds (VOCs) and explosives. We have found that **14** (Scheme 9) can be used for VOC detection.[40] A deposit of **14** on a thin-layer chromatography (TLC) plate is strongly emissive, but the light emission is turned off after exposure of the TLC plate to chloroform vapor. The emission can be recovered after the vapor is removed. Such fluorescence switching can be attributed to the liquid formation of the solvent on the TLC plate and as a result the thin layer coating of **14** on the TLC plate is dissolved, leading to fluorescence quenching. Similar fluorescence variation for **14** is observed for other VOCs such as acetone, dichloromethane, acetonitrile and THF.

Silole and TPE luminogens have also been explored as chemosensors for explosives such as 2,4-dinitrotoluene (DNT), 2,4,6-trinitrotoluene (TNT) and picric acid (PA). We have recently reported the synthesis of polymers **15** containing TPE

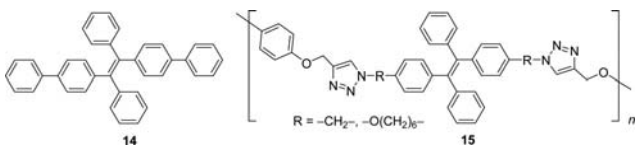

Scheme 9 AIE luminogen **14** and polymer **15** containing TPE units for the detections of VOCs and explosives.

units (Scheme 9) and their applications in detection of PA.[41] The polymers are still AIE active: they are non-fluorescent in solution but become strongly emissive after aggregation. The strong fluorescence of the nanoaggregates of **15** can be quenched by addition of PA. Both energy transfer and super-quenching have contributed to the fluorescence reduction after addition of PA. Moreover, a prototype device for the detection of explosives has been demonstrated based on thin films of **15**. Apart from the TPE luminogens, silole and its oligomers have also been investigated for detection of explosives.[42]

Conclusion and perspective

Since the discovery of the AIE phenomenon of **1** in 2001,[4] extensive research has been devoted to the syntheses of AIE-active luminogens and exploration of their applications. As a result, a large number of new AIE luminogens have been designed and synthesized, and the restriction of intramolecular rotation has been identified as the main cause for the AIE effect. The abnormal emissive feature of the AIE luminogens differentiates them from "conventional" luminophores. Many application possibilities can be imaged for the AIE systems. Among them, the utilization of AIE luminogens to fabricate efficient OLEDs and to develop new bio/chemosensors has already offered promising results. In this short review, we mainly summarized the recent progress in the development of AIE-based bio/chemosensors. These include: 1) detection of charged biomacromolecules, 2) nuclease and AChE activity assay as well as inhibitor screening, 3) selective detection of specific anions and metal cations, and 4) detection of VOCs and explosives.

Traditional fluorophores experience emission quenching in concentrated solutions and solid aggregates, and accordingly fluorescent sensors based on these fluorophores usually suffer from the following limitations: 1) fluorophores can be used only at low concentrations, which may reduce their sensitivities and 2) most of these sensors cannot be used in aqueous solutions as the fluorophores would aggregate in water, leading to fluorescence quenching. In sharp contrast, fluorescent sensors based on AIE molecules can overcome these limitations: 1) the AIE feature permits the use of concentrated solutions and aggregate suspensions in the aqueous media for sensing applications, 2) the solutions of AIE molecules are strongly emissive, sensitive and photobleaching-resistant, and 3) label-free biosensors can be established with AIE molecules. These advantages will enable us to realize fluorescence turn-on detection of biomolecules and on-site, label-free enzyme assays as well as high-throughout inhibitor screening that has important implications for drug discovery.

Apart from silole and TPE derivatives, other AIE-active molecules such as a lambda-shaped pyridinium salt[43] and a phosphorus compound[44] have been also investigated for the detection of proteins and explosive compounds, chiral recognition[45] and as probes for sugar-protein interaction. Application of AIE-active starburst triarylamine fluorophores for gas sensing has also been described.[46]

It should be noted that the AIE effect is also relevant to bioluminescence systems. For instance, the steric hindrance experienced by the chromophore within the native green fluorescent protein (GFP) prevents the *cis-trans* rotational isomerization, which confers strong emissive behavior on the protein.[47] Also, aggregation occurs in many biological processes. Therefore, it may be concluded that application of AIE luminogens as biosensors is just a beginning and many possibilities await exploration. Bioimaging with AIE molecules may deserve particular attention. In these regards, the development of new AIE luminogens that emit at long wavelengths (*e.g.* in the near-infrared region) and new strategies for linking specific recognition groups to the AIE luminogens should be the key points for further research in this area.

Acknowledgements

This work was supported by the National Science Foundation of China, the Ministry of Science and Technology, the Chinese Academy of Sciences, and the Research Grants Council of Hong Kong (603509 and 603008).

Notes and references

1 See, for example, (*a*) R. H. Friend, R. W. Gymer, A. B. Holms, J. H. Burroughes, R. N. Marks, C. Taliani, D. D. C. Bradley, D. A. Dos Santos, J. L. Brédas, M. Lögdlund and W. R. Salaneck, *Nature*, 1999, **397**, 121; (*b*) S. A. Jenekhe and J. A. Osaheni, *Science*, 1994, **265**, 765.
2 See, for example, (*a*) D. W. Domaille, E. L. Que and C. J. Chang, *Nat. Chem. Biol.*, 2008, **4**, 168; (*b*) M. H. Lim and S. J. Lippard, *Acc. Chem. Res.*, 2007, **40**, 41; (*c*) B. N. G. Giepmans, S. R. Adams, M. H. Ellisman and R. Y. Tsien, *Science*, 2006, **312**, 217.
3 See, for example, E. A. Jares- Erijman and T. M. Jovin, *Nat. Biotechnol.*, 2003, **21**, 1387.
4 J. D. Luo, Z. L. Xie, J. W. Y. Lam, L. Cheng, H. Y. Chen, C. F. Qiu, H. S. Kwok, X. W. Zhan, Y. Q. Liu, D. B. Zhu and B. Z. Tang, *Chem. Commun.*, 2001, 1740. For more recent reviews, see: (*a*) Y. N. Hong, J. W. Y. Lam and B. Z. Tang, *Chem. Commun.*, 2009, 4332; (*b*) J. Liu, J. W. Y. Lam and B. Z. Tang, *J. Inorg. Organomet. Polym. Mater.*, 2009, **19**, 249.
5 H. Tong, Y. N. Hong, Y. Q. Dong, M. Haussler, J. W. Y. Lam, Z. Li, Z. F. Guo, Z. H. Guo and B. Z. Tang, *Chem. Commun.*, 2006, 3705.
6 G. Yu, S. Yin, Y. Liu, J. Chen, X. Xu, X. Sun, D. Ma, X. Zhan, Q. Peng, Z. Shuai, B. Z. Tang, D. Zhu, W. Fang and Y. Luo, *J. Am. Chem. Soc.*, 2005, **127**, 6335.
7 (*a*) B. Z. Tang, X. W. Zhan, G. Yu, P. P. S. Lee, Y. Q. Liu and D. B. Zhu, *J. Mater. Chem.*, 2001, **11**, 2974; (*b*) J. W. Chen, C. C. W. Law, J. W. Y. Lam, Y. P. Dong, S. M. F. Lo, I. D. Williams, D. B. Zhu and B. Z. Tang, *Chem. Mater.*, 2003, **15**, 1535.
8 Y. Q. Dong, J. W. Y. Lam, A. Qin, Z. Li, J. Z. Liu, J. Z. Sun, Y. P. Dong and B. Z. Tang, *Chem. Phys. Lett.*, 2007, **446**, 124.
9 M. Wang, D. Q. Zhang, G. X. Zhang and D. B. Zhu, *Chem. Commun.*, 2008, 4469.
10 M. Wang, D. Q. Zhang, G. X. Zhang, Y. L. Tang, S. Wang and D. B. Zhu, *Anal. Chem.*, 2008, **80**, 6443.
11 M. Wang, X. G. Gu, G. X. Zhang, D. Q. Zhang and D. B. Zhu, *Anal. Chem.*, 2009, **81**, 4444.
12 L. H. Peng, G. X. Zhang, D. Q. Zhang, J. F. Xiang, R. Zhao, Y. L. Wang and D. B. Zhu, *Org. Lett.*, 2009, **11**, 4014.
13 L. H. Peng, M. Wang, G. X. Zhang, D. Q. Zhang and D. B. Zhu, *Org. Lett.*, 2009, **11**, 1943.
14 S. J. Toal, K. A. Jones, D. Magde and W. C. Trogler, *J. Am. Chem. Soc.*, 2005, **127**, 11661.
15 L. Liu, G. X. Zhang, J. F. Xiang, D. Q. Zhang and D. B. Zhu, *Org. Lett.*, 2008, **10**, 4581.
16 (*a*) D. L. Rabenstein, *Nat. Prod. Rep.*, 2002, **19**, 312; (*b*) J. Hirsh, J. E. Dalen, D. Deykin and L. Poll, *Chest*, 1992, **102**, 337S.
17 I. Caplia and R. J. Linhardt, *Angew. Chem., Int. Ed.*, 2002, **41**, 390.
18 H. Tong, Y. N. Hong, Y. Q. Dong, M. Haeussler, Z. Li, J. W. Y. Lam, Y. P. Dong, H. H. Y. Sung, I. D. Williams and B. Z. Tang, *J. Phys. Chem. B*, 2007, **111**, 11817.

19 Y. N. Hong, M. Haussler, J. W. Y. Lam, Z. Li, K. K. Sin, Y. Q. Dong, H. Tong, J. Z. Liu, A. J. Qin, R. Renneberg and B. Z. Tang, *Chem.–Eur. J.*, 2008, **14**, 6428.
20 (*a*) J. T. Davis, *Angew. Chem., Int. Ed.*, 2004, **43**, 668; (*b*) N. Maizels, *Nat. Struct. Mol. Biol.*, 2006, **13**, 1055; (*c*) S. Neidle and G. Parkinson, *Nat. Rev. Drug Discovery*, 2002, **1**, 383.
21 (*a*) M.-P. Teulade-Fichou, C. Carrasco, L. Guittat, C. Bailly, P. Alberti, J.-L. Mergny, A. David, J.-M. Lehn and W. D. Wilson, *J. Am. Chem. Soc.*, 2003, **125**, 4732; (*b*) S. Nakayama and H. O. Sintim, *J. Am. Chem. Soc.*, 2009, **131**, 10320.
22 (*a*) P. Prentø, *Biotech. Histochem.*, 2001, **76**, 137; (*b*) A. Granzhan and H. Ihmels, *Org. Lett.*, 2005, **7**, 5119; (*c*) A. Granzhan, H. Ihmels and G. Viola, *J. Am. Chem. Soc.*, 2007, **129**, 1254.
23 S. M. Linn and R. J. Roberts, *Nucleases*, Cold Spring Harbor Labortary Press: Cold spring Harbor, NY, 1982.
24 K. T. Bush, S. H. Keller and S. K. Nigam, *J. Clin. Invest.*, 2000, **106**, 621.
25 S. Przedborski and M. Vila, *Clin. Neurosci. Res.*, 2001, **1**, 407.
26 M. Zhao, M. Wang, D. Liu, G. Zhang, D. Zhang and D. Zhu, *Langmuir*, 2009, **25**, 676–678.
27 P. J. Whitehouse, D. L. Price, R. G. Struble, A. W. Clark, J. T. Coyle and M. R. Delon, *Science*, 1982, **215**, 1237.
28 H. D. Chen, X. L. Zuo, S. Su, Z. Z. Tang, A. B. Wu, S. P. Song, D. B. Zhang and C. H. Fan, *Analyst*, 2008, **133**, 1182.
29 S. Su, Y. He, M. Zhang, K. Yang, S. Song, X. Zhang and C. H. Fan, *Appl. Phys. Lett.*, 2008, **93**, 023113.
30 (*a*) F. D. Feng, Y. L. Tang, S. Wang, Y. L. Li and D. B. Zhu, *Angew. Chem., Int. Ed.*, 2007, **46**, 7882; (*b*) S. Sabelle, P. Y. Renard, K. Pecorella, S. De Suzzoni-Dezard, C. Creminon, J. Grassi and C. Mioskowski, *J. Am. Chem. Soc.*, 2002, **124**, 4874.
31 See, for example, M. Wang, X. G. Gu, G. X. Zhang, D. Q. Zhang and D. B. Zhu, *Langmuir*, 2009, **25**, 2504.
32 See, for example, R. Gill, L. Bahshi, B. Freeman and I. Willner, *Angew. Chem., Int. Ed.*, 2008, **47**, 1676.
33 T. Moczoń and A. Swietlikoowska, *Acta. Parasitological.*, 2005, **50**, 344.
34 A. G. Hadd, S. C. Jacobson and J. M. Ramsey, *Anal. Chem.*, 1999, **71**, 5206.
35 M. Harel, I. Schalk, L. Ehret-Sabatier, F. Bouet, M. Goeldner, C. Hirth, P. H. Axelsen, I. Silman and J. L. Sussman, *Proc. Natl. Acad. Sci. U. S. A.*, 1993, **90**, 9031.
36 B. Vennesland, E. E. Comm, C. J. Knownles, J. Westly and F. Wissing, *Cyanide in Biology*; Academic Press: London, 1981.
37 (*a*) J. L. Sessler and D.-G. Cho, *Org. Lett.*, 2008, **10**, 73; (*b*) W. Todd and F. P. Gabba, *J. Am. Chem. Soc.*, 2007, **129**, 11978; (*c*) X. D. Lou, L. Y. Zhang, J. G. Qin and Z. Li, *Chem. Commun.*, 2008, 5848.
38 E. M. Nolan and S. J. Lippard, *Chem. Rev.*, 2008, **108**, 3443 and references therein.
39 (*a*) A. Coskun and E. U. Akkaya, *J. Am. Chem. Soc.*, 2005, **127**, 10464; (*b*) E. M. Nolan and S. J. Lippard, *J. Am. Chem. Soc.*, 2007, **129**, 5910; (*c*) B. Liu and H. Tian, *Chem. Commun.*, 2005, 3156.
40 Y. Dong, J. W. Y. Lam, A. Qin, J. Liu, Z. Li, B. Z. Tang, J. Sun and H. S. Kwok, *Appl. Phys. Lett.*, 2007, **91**, 011111.
41 (*a*) Z. Li, Y. Dong, B. X. Mi, Y. H. Tang, M. Haussler, H. Tong, Y. P. Dong, J. W. Y. Lam, Y. Ren, H. H. Y. Sung, K. S. Wong, P. Gao, I. D. Williams, H. S. Kwok and B. Z. Tang, *J. Phys. Chem. B*, 2005, **109**, 10061; (*b*) A. J. Qin, J. W. Y. Lam, L. Tang, C. K. W. Jim, H. Zhao, J. Z. Sun and B. Z. Tang, *Macromolecules*, 2009, **42**, 1421.
42 (*a*) H. Sohn, R. M. Calhoun, M. J. Sailor and W. C. Trogler, *Angew. Chem., Int. Ed.*, 2001, **40**, 2104; (*b*) H. Sohn, M. J. Sailor, D. Magde and W. C. Trogler, *J. Am. Chem. Soc.*, 2003, **125**, 3821.
43 C. X. Yuan, X. T. Tao, L. Wang, J. X. Yang and M. H. Jiang, *J. Phys. Chem. C*, 2009, **113**, 6809.
44 T. Sanji, K. Shiraishi and M. Tanaka, *ACS Appl. Mater. Interfaces*, 2009, **1**, 270.
45 Y. S. Zheng and Y. J. Hu, *J. Org. Chem.*, 2009, **74**, 5660.
46 Z. J. Ning, Z. Chen, Q. Zhang, Y. L. Yan, S. X. Qian, Y. Cao and H. Tian, *Adv. Funct. Mater.*, 2007, **17**, 3799.
47 J. Dong, K. M. Solntsev and L. M. Tolbert, *J. Am. Chem. Soc.*, 2009, **131**, 662.